Lasing from semiconductor microring on the end of an optical fiber

B. Corbett and P. LambkinG. H. Wu, J. Houlihan, and G. Huyet

Citation: Appl. Phys. Lett. **81**, 808 (2002); doi: 10.1063/1.1496496
View online: http://dx.doi.org/10.1063/1.1496496
View Table of Contents: http://aip.scitation.org/toc/apl/81/5
Published by the American Institute of Physics

Lasing from semiconductor microring on the end of an optical fiber

B. Corbett[a] and P. Lambkin
National Microelectronics Research Centre, University College Cork, Prospect Row, Cork, Ireland

G. H. Wu, J. Houlihan, and G. Huyet
Physics Department, National University of Ireland, University College, Cork, Ireland

(Received 8 January 2002; accepted for publication 3 June 2002)

Isolated InGaAsP microrings with an outer diameter of 5.8 μm, a width of 1 μm, and a thickness of 0.41 μm were fabricated by epitaxial separation. Individual devices were bonded to multimode optical fiber using Van der Waals forces and optically pumped through the fiber. Lasing around 1505 nm was measured under pulsed and cw pumping at room temperature. The threshold pump power for pulsed operation was estimated to be 38 and 80 μW for cw operation. Multiple radial and azimuthal modes were present due to strong, three-dimensional confinement. Under strong pulsed pumping thermal effects caused the emission wavelength to chirp. © *2002 American Institute of Physics.* [DOI: 10.1063/1.1496496]

Compact components such as microdisks[1–7] and microrings[8,9] are expected to find applications in high density, optically interconnected systems both for active and passive functions. Their high Q resonances combined with small volumes leads to small thresholds whether for lasing or switching and, hence, the possibility for realizing large arrays without excessive power dissipation. The reduction in the scale of the mode volume towards that of an optical wavelength also leads to interesting physical effects such as an increase in the spontaneous emission factor[7] and the possibility of thresholdless lasing. In order to exploit these, practical systems and applications will need to function at a useful wavelength range (e.g., 1500 nm for telecommunications) and under room temperature conditions.

Microdisks have been previously fabricated using a supporting pillar to provide the dielectric contrast that favors the whispering gallery modes. However, this method makes coupling to the disks nontrivial requiring precise positioning of pump beams or connecting probes. In addition thermal heat sinking is problematic in this geometry. There are alternative techniques using substrate removal[3,5,8] and attaching the microdisks to a low refractive index surface. This improves the heat sinking and permits the use of different cavity geometries such as microrings. We extend this approach here by fabricating free standing, microring and microdisk devices that are then individually placed on the end facet of an optical fiber. This permits a simple pumping geometry and facilitates the study of individual devices. In this letter we report on the fabrication and cw lasing characteristics of such uncooled microring lasers.

Epitaxial layers were grown by metalorganic chemical vapor deposition on an InP substrate. They consisted of four, 5 nm, compressively strained, InGaAsP quantum wells sandwiched between 180 nm of InGaAsP cladding ($\lambda_g = 1.16$ μm). All the layers were undoped to reduce free carrier losses. On the substrate the quantum wells showed a photoluminescence peak at 1482 nm. The total thickness of the epilayers was 410 nm which, when separated and bounded by glass ($n=1.46$) and air ($n=1$), can support two in-plane guided modes. The effective index of the fundamental guided mode was calculated as 3.11 at $\lambda = 1500$ nm. The modal confinement factor, Γ, within the quantum wells was 0.02, similar to conventional edge emitting lasers. The mode was mostly confined within the slab unlike thinner structures.[1,7] The first order transverse mode is not expected to play any role due to the zero overlap, Γ, with the quantum wells.

The devices were fabricated using optical lithography to define separate arrays of rings and disks in the 4–20 μm outer diameter range. Mesas were etched to a depth >1 μm using a nonselective and noncrystallographic $HBr:H_3PO_4:K_2CrO_7$ based etchant. This is an important step as it leads to smooth etched surfaces. The mesas were then covered in wax and the InP substrate removed selectively in concentrated HCl. The individual arrays of a given diameter were separated and the wax removed before individual devices were released onto filter paper. An individual device could then be placed on the end of a 50 μm diameter core multimode optical fiber using water and the resultant Van der Waals forces. Despite the small dimensions (typically

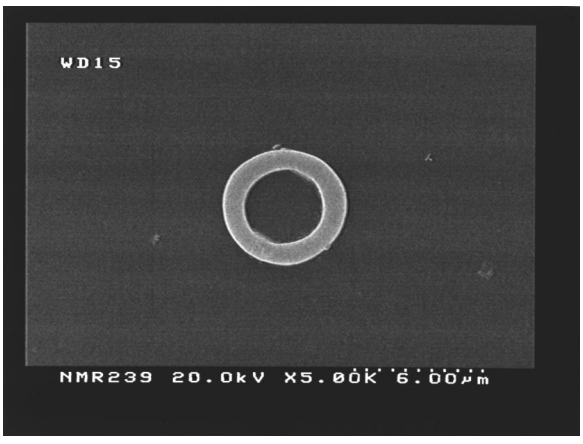

FIG. 1. Scanning electron micrograph image of microring attached to a multimode optical fiber. The outer diameter of the ring is 5.8 μm and the inner diameter is 3.7 μm with the width of the ring being 1 μm.

[a]Electronic mail: bcorbett@nmrc.ie

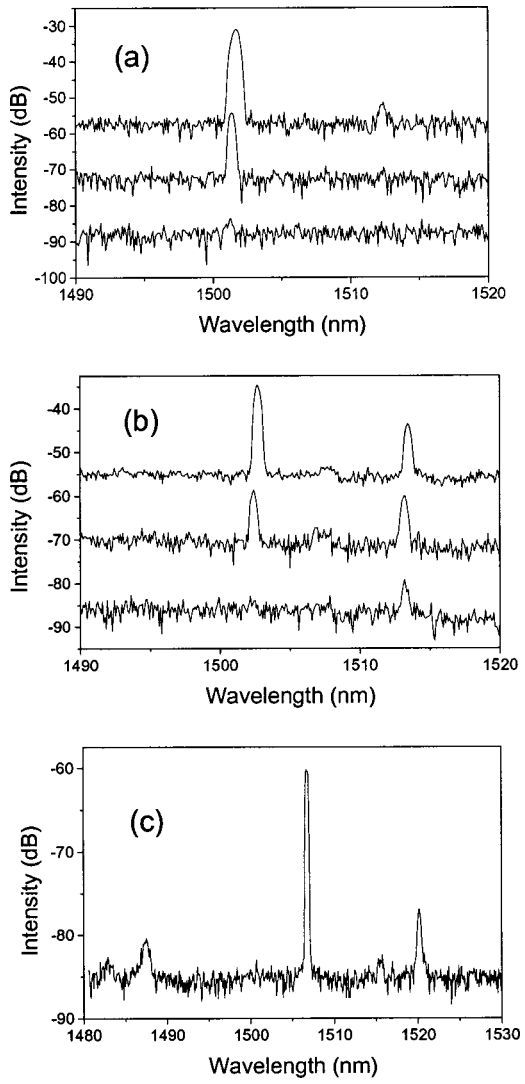

FIG. 2. Spectra from microring undera pulsed and (b) cw pumping. The estimated absorbed pump power in the pulse case is 31, 58, and 154 μW while in the cw regime it is 50, 85, and 115 μW. The resolution of the spectrometer is set to be 0.5 nm. The spectrum from a second disk is shown in (c) under cw pumping with power of 110 μW. Note the change in scale in (c).

0.4 μm$\times$6 μm$\times$6 μm) the devices are very robust. The manual placement accuracy of $+/-15$ μm can be improved with more refined techniques. Figure 1 shows a scanning electron microscopy image of a bonded device. The outer diameter is 5.8 μm and the inner diameter is 3.7 μm.

The devices were optically pumped through the fiber with a 980 nm laser under pulsed and cw conditions. The emission from the ring was collected at approximately 30° with a cleaved multimode fiber connected to an optical spectrum analyzer. The unused pump power, P_{out}, from the fiber was also measured and the absorbed power in the ring is estimated by taking the ratio of the device area to the fiber core area and including the absorption in the epilayers and the fiber to semiconductor reflectivity.

Figure 2(a) shows the evolution of the luminescence spectrum from the ring under pulsed pumping conditions while Fig. 2(b) shows the evolution under cw conditions. Under pulsed conditions (100 ns pulse at 1 kHz) the threshold pump power is estimated to be 38 μW (note this corresponds to approximately 10 mW through fiber) and the

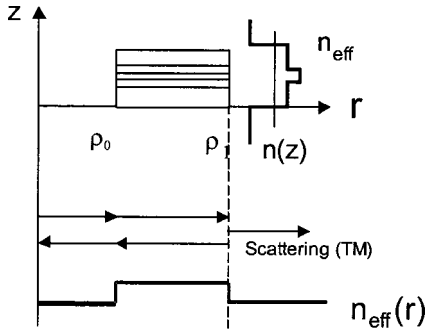

FIG. 3. The effective index, scattering method applied to a microcavity ring resonator. An effective index calculation first removes any dependency on the z coordinate. A cylindrical wave is then considered incident on the cavity's inner surface. The intensity of the wave escaping from the outer surface is calculated by applying appropriate boundary conditions. It is found to be a resonant function of wavelength.

power as measured by the integrated spectrum increases linearly with pumping. The lasing mode is at 1501.5 nm. Under cw conditions the threshold has increased to 80 μW and is lasing in two modes at 1502.3 and 1513.3 nm. The 0.8 nm shift in mode location under cw is due to the temperature dependence of the refractive index (2×10^{-4}/K) and corresponds to an increase in temperature in the active region of 8 K. Figure 2(c) shows the lasing spectrum from a second disk with the same nominal dimensions. In addition to the prominent mode at 1507 nm, other modes are measured at 1487, 1516, and 1520 nm. While the precise spectral locations are different for the different rings the general form is similar.

The modes of the ring cavity have been calculated using a scattering matrix technique[10,11] that involves applying the effective index approximation. It follows the analysis usually employed for rectangular geometry laser resonators. For example, to formally obtain the lasing spectrum for a ridge waveguide laser the effective index (EI) method is first applied to obtain an ''effective'' index. The longitudinal laser modes then correspond to the Fabry–Perot transmission resonances of a dielectric slab with the index obtained from the EI calculation and a thickness corresponding to the laser length. The same methodology can be applied to the ring cavity as illustrated in Fig. 3. The ''slab waveguide'' is first solved for the TE mode at a given wavelength. This yields an effective index that is now assumed to be infinite in extent along the z axis. The annular nature of the cavity leads to an effective ''hollow'' fiber. A cylindrical wave radiation source is then considered to be located along the z axis. By applying appropriate boundary conditions a TM scattering matrix is used to establish the transmission external to the cavity. The incident and reflected waves are treated as traveling wave, Hankel functions in the radial direction, whilst the azimuthal distribution is given by $e^{im\phi}$, where, m, is an integer. Transmission resonances then correspond to the possible lasing wavelengths.

The resonant modes of a 6 μm diameter ring cavity with a 4 μm diameter air core have been calculated using the method outlined earlier. Unlike the relatively large Fabry–Perot laser cavities, modal and material dispersion characteristics become significant in microcavities and have been included in the calculations. In Fig. 4 the radial mode order (number of intensity minima in the radial direction) has been

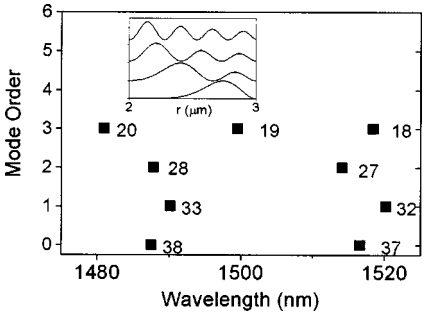

FIG. 4. Azimuthal mode wavelengths for a 6 μm diameter microcavity ring resonator with a width of 1 μm. Inset: The normalized radial intensity distributions across the ring width for the radial order 0–3.

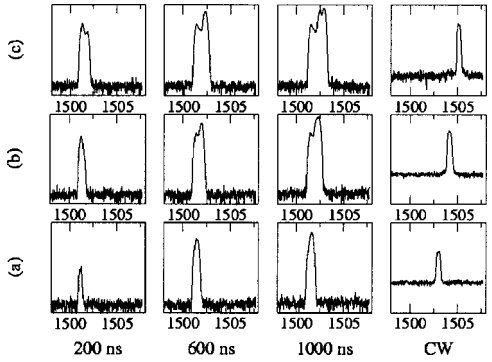

FIG. 5. Evolution of lasing mode from the microring as the device is pumped with increasing pulse duration (200, 600, 1000, and cw) and increased optical power. The estimated absorbed optical power was 150, 200, and 250 μW in (a), (b), and (c), respectively. The spectrometer resolution was 0.2 nm.

plotted against the wavelength position of the modes and labeled with the azimuthal mode number "m."

Due to the strong refractive confinement and despite the small width (1 μm) of the ring, several radial modes are lasing. We identify the strongest mode around 1502 nm (ring 1), 1507 nm (ring 2) with the third order mode $m=19$ (Fig. 4). The lower Q of this mode is compensated by the increased spatial overlap (Fig. 4 inset) of the mode with the gain region and the better match to the gain peak. The modes at longer wavelength (ring 1 and 2) are identified with the fundamental radial mode ($m=37$) while the shorter wavelength modes seen in ring 2 correspond to $m=33$ and $m=38$.

The threshold power P_{th} in pulsed operation was 38 μW corresponding to a pump density of 250 W/cm^2. An equivalent threshold current density of 300 A/cm^2 can be derived and is similar to previous results.[7] The threshold is determined by the carrier density required for achieving transparency and additionally overcoming the losses associated with the waveguide and mirrors. As the layers are undoped and all the modes have a high Q as seen by the lasing of a third order mode, it is the transparency condition that dominates. Unlike microdisks formed on a supporting pedestal there are no additional parasitic losses for high order modes. However, reabsorption of spontaneous emission in the highly confined dielectric structure, and the spontaneous emission factor reduce this value.

In order to study the lasing characteristics under high pump levels, pump light was focused directly onto the ring (instead of through the optical fiber) in both pulsed and cw regimes. Interestingly, changing the pulse width from 200 to 1000 ns with fixed power (or increasing the pump power with fixed pulse width) caused each lasing wavelength to experience a redshift while broadening (Fig. 5). Since this shift occurs for changes in both the pump level and pulse width it can be associated with thermal effects. The fact that this broadening does not appear under cw pumping indicates that it is a transient phenomenon. Thus, the broadening is the result of a transient redshift of the lasing mode. This mode chirping which is seen under strong pumping may limit the use of such devices for applications requiring switching.

In summary, we have demonstrated lasing action in a compact microring resonator positioned in a configuration using a simple fabrication process. Room temperature cw lasing has been measured in all the devices tested. High order modes dominate the lasing characteristics and a reduction of the width of the microring will be required to eliminate the high order radial modes. It may be possible to integrate these devices with single mode fiber and permit more efficient coupling to the pump beam.

This work was supported by Enterprise Ireland Project No. SC/98/750.

[1] S. L. McCall, A. F. J. Levi, R. E. Slusher, S. J. Pearton, and R. A. Logan, Appl. Phys. Lett. **60**, 289 (1992).
[2] R. E. Slusher, A. F. J. Levi, U. Mohideen, S. L. McCall, S. J. Pearton, and R. A. Logan, Appl. Phys. Lett. **63**, 1310 (1993).
[3] B. Corbett, J. Justice, L. Considine, S. Walsh, and W. M. Kelly, IEEE Photonics Technol. Lett. **8**, 855 (1996).
[4] W. G. Bi, Y. Ma, J. P. Zhang, L. W. Wang, S. T. Ho, and C. W. Tu, IEEE Photonics Technol. Lett. **9**, 1072 (1997).
[5] S. M. K. Thiyagarajan, A. F. J. Levi, C. K. Lin, I. Kim, P. D. Dapkus, and S. J. Pearton, Electron. Lett. **34**, 2333 (1998).
[6] S. M. K. Thiyagarajan, D. A. Cohen, A. F. J. Levi, C. S. Ryu, R. Li, and P. D. Dapkus, Electron. Lett. **35**, 1252 (1999).
[7] M. Fujita, K. Teshima, and T. Baba, Jpn. J. Appl. Phys., Part 2 **40**, L875 (2001).
[8] B. Corbett, IEEE Photonics Technol. Lett. **10**, 3 (1998).
[9] K. C. Zeng, L. Dai, J. Y. Lin, and H. X. Jiang, Appl. Phys. Lett. **75**, 2563 (1999).
[10] D. Rafizadeh, J. P. Zhang, R. C. Tiberio, and S. T. Ho, J. Lightwave Technol. **16**, 1308 (1998).
[11] M. Born and E. Wolf, *Principles of Optics*, 7th ed. (CUP, Cambridge, 1999).